DEUTSCHES ELEKTRONEN – SYNCHROTRON

DESY 93-012
February 1993

Supersymmetric Threshold Corrections to the Higgs Sector in the Minimal Supersymmetric Model

R. Hempfling

Deutsches Elektronen-Synchrotron DESY, Hamburg

ISSN 0418-9833

NOTKESTRASSE 85 · D-2000 HAMBURG 52

To be sure that your preprints are promptly included in the
HIGH ENERGY PHYSICS INDEX,
send them to (if possible by air mail):

DESY **Bibliothek** **Notkestraße 85** **W-2000 Hamburg 52** **Germany**	**DESY-IfH** **Bibliothek** **Platanenallee 6** **O-1615 Zeuthen** **Germany**

DESY 93-012
February 1993

ISSN 0418-9833

Supersymmetric Threshold Corrections to the Higgs Sector in the Minimal Supersymmetric Model

R. HEMPFLING*

Deutsches Elektronen-Synchrotron, Notkestraße 85, 2000 Hamburg 52, Germany

ABSTRACT

In the minimal supersymmetric extension of the Standard Model (MSSM), the Higgs self-interactions are related to the $SU(2)_L \times U(1)_Y$ gauge couplings. Thus, only two additional inputs are needed in order to completely determine the Higgs sector of the theory. However, these relations acquire radiative corrections when supersymmetry (SUSY) is broken. In this paper, we investigate the phenomenological implications of the corrections due to trilinear Higgs-squark-squark interactions.

1. Introduction

The relations between the $SU(2)_L \times U(1)_Y$ gauge couplings and the quartic Higgs self-coupling in the MSSM yield a very restrictive Higgs sector at tree-level. Only two additional inputs (typically chosen to be the ratio of vacuum expectation values, $\tan\beta$, and the mass of the CP-odd scalar, m_{A^0}) completely determine the Higgs sector of the theory. However, it has recently been found that one-loop radiative corrections can significantly alter the tree-level predictions[1-10]. The reason is that the dominant radiative corrections grow logarithmically with the SUSY breaking scale, M_{SUSY}. The effects of these leading log terms have been studied in detail[11-16]. In this paper we present the effects of non-logarithmic corrections generated at the SUSY threshold. These types of corrections can be important in cases where the leading log terms are small or absent. For example, consider the case of large $\tan\beta$ and $m_{A^0} \lesssim m_Z$. In this limit, the Higgs masses are given by

$$m_{H^0} = m_Z \qquad \text{and} \qquad m_{h^0} = m_{A^0} \,. \tag{1}$$

While the first relation acquires very large radiative corrections, [of the order of $g_2^2 m_t^4/m_Z^2 \ln(M_t^2/m_t^2)$] the second relation remains unchanged at the leading log level.

* Talk presented at the 23rd Workshop of the INFN ELOISATRON Project "PROPERTIES OF SUSY PARTICLES", Erice-Italy, September 28 - October 4, 1992.

In the MSSM, the Higgs production via $Z \to Z^* h^0$ is suppressed by a factor of $\sin^2(\beta-\alpha)$. This factor vanishes in the limit $\tan\beta \to \infty$ in the case where $m_{A^0} < m_Z$. In this limit, the Higgs bosons can be searched for via the complimentary process $Z \to h^0 A^0$ where the decay rate is proportional to $\cos^2(\beta-\alpha)$. Non-observation of the latter process implies $m_{A^0} + m_{h^0} \gtrsim m_Z$. This together with Eq. (1) has been used in refs. 17–19 to set a lower limit of 41 GeV ($\approx m_Z/2$) on the lightest Higgs mass of the MSSM. In the next section, we will incorporate the full one-loop radiative corrections into this analysis.

2. The Experimental Lower Limit of m_{h^0} in the MSSM

In this section, we would like to demonstrate that non-logarithmic corrections can alter the Higgs phenomenology of the MSSM significantly.

At tree-level, A^0 and h^0 are mass degenerate. This relation acquires corrections when loop effects are included. We obtain the following relation among the one-loop radiatively corrected Higgs boson masses defined as the pole of the propagator

$$(\Delta m_0^2)_{\beta=\pi/2} \equiv m_{A^0}^2 - m_{h^0}^2 = \mathrm{Re}\left[A_{A^0A^0}(m_{h^0}^2) - A_{h^0h^0}(m_{h^0}^2)\right] . \tag{2}$$

The subscript $(\beta = \pi/2)$, indicating that our result is only valid in this particular case, is suppressed from now on. In our notation, $-iA_{SS}(p^2)$ $(S = h^0, A^0)$ denotes the sum of all one–loop Feynman graphs contributing to the scalar two-point functions (p is the four-momentum of one of the external legs). Note that in the derivation of Eq. (2) we have assumed that $m_{A^0} \lesssim m_Z$. The analogous result for the case $m_{A^0} \gtrsim m_Z$ is obtained by replacing $h^0 \to H^0$. With Eq. (2) and the experimental lower bound on the sum $m_{A^0} + m_{h^0} \geq m_Z$ from the non-observation of the decay $Z \to h^0 A^0$, we can now derive rough lower bounds on the individual Higgs masses

$$\begin{aligned} m_{A^0} &\geq \tfrac{1}{2} m_Z + (\Delta m_0) \,, \\ m_{h^0} &\geq \tfrac{1}{2} m_Z - (\Delta m_0) \,, \end{aligned} \tag{3}$$

where the linear mass shift is defined as $(\Delta m_0) \equiv (\Delta m_0^2)/(2m_Z)$. Eq. (3) is the main result of this section. It can be generalized to the process $Z^* \to A^0 h^0$ with an arbitrary CM-energy $\sqrt{s}$ by the substitution $m_Z \to \sqrt{s}$.

We now turn to the numerical evaluation of the A^0—h^0 mass shift. First we note that the Higgs potential is invariant under two U(1) symmetries in the large $\tan\beta$ limit corresponding to individual phase rotations of the two Higgs doublets. One combination of these symmetries is gauged [namely $U(1)_Y$] whereas the other one is the global symmetry $U(1)_g$ which guarantees the A^0—h^0 mass degeneracy. We therefore start our numerical analysis by identifying those terms of the Lagrangian that break $U(1)_g$ explicitly.

By inspecting the Lagrangian, we find that $U(1)_g$ is broken in the Higgs-Higgsino sector via

$$\begin{aligned} \mathcal{V}_H &= -m_{12}^2 H_1^* H_2 + \text{h.c.}\,, \\ \mathcal{V}_{\widetilde{H}} &= -\mu \widetilde{H}_1 \epsilon \widetilde{H}_2 + \text{h.c.}\,, \end{aligned} \tag{4}$$

and in the squark sector via a combination of the F-terms and the A parameters

$$\begin{aligned} \mathcal{V}_F &= -\mu \left[h_U \left(H_1^\dagger \widetilde{Q} \right) \widetilde{U} + h_D \left(H_2^\dagger \widetilde{Q} \right) \widetilde{D} + \text{h.c.} \right], \\ \mathcal{V}_A &= -h_U A_U \left(i H_2^T \sigma_2 \widetilde{Q} \right) \widetilde{U} + h_D A_D \left(i H_1^T \sigma_2 \widetilde{Q} \right) \widetilde{D} + \text{h.c.} \end{aligned} \tag{5}$$

where $\widetilde{Q}$ ($\widetilde{U}, \widetilde{D}$) stands for the left-handed (right-handed) squark fields. Here the Yukawa couplings of the up and down type quarks are related to the masses via

$$h_U = \frac{g_2 m_U}{\sqrt{2} m_W \sin\beta}, \qquad h_D = \frac{g_2 m_D}{\sqrt{2} m_W \cos\beta}. \tag{6}$$

Furthermore, in the large $\tan\beta$ limit we have $m_{12}^2 \to 0$. Thus, we can conclude that the only significant contributions to $m_{A^0} - m_{h^0}$ can come from the gaugino-Higgsino sector and the top- and the bottom-squark sector (notice that in the large $\tan\beta$ limit the bottom Yukawa coupling must become large if m_b is fixed at its observed value).

Before presenting the numerical results, we first choose a suitable parameterization. In the squark sector it is very convenient to present the results as functions of the squark mass eigenvalues M_i ($i = \tilde{t}_1, \tilde{t}_2, \tilde{b}_1, \tilde{b}_2$) and the trilinear coupling constants (A_t and μ). This parameterization is subject to the constraint

$$m_t A_t \leq \left| M_{\tilde{t}_1}^2 - M_{\tilde{t}_2}^2 \right|. \tag{7}$$

However, this choice has various advantages. First, the parameters are physical quantities and experimental constraints can readily be imposed. Second, the expressions for the top- and bottom-squark contributions are equivalent: all one needs to do is to replace the Yukawa couplings ($h_t \to h_b$), $A_t^2 \to \mu^2$ and $\mu^2 \to A_b^2$. Third, the most important advantage is the factorization of the result. It can be written as

$$(\Delta m_0)^{\tilde{t}} = 1.92\,\text{GeV} \left(\frac{m_t}{2 m_Z} \right)^4 \left(\frac{2\mu^2}{M_{\tilde{t}_1}^2 + M_{\tilde{t}_2}^2} \right) \left(\frac{2A_t^2}{M_{\tilde{t}_1}^2 + M_{\tilde{t}_2}^2} \right) G(M_{\tilde{t}_1}^2, M_{\tilde{t}_2}^2, m_{h^0}^2). \tag{8}$$

The definition of the function G is given in Appendix A. Here we just present the asymptotic expansion of G in the large squark mass limit

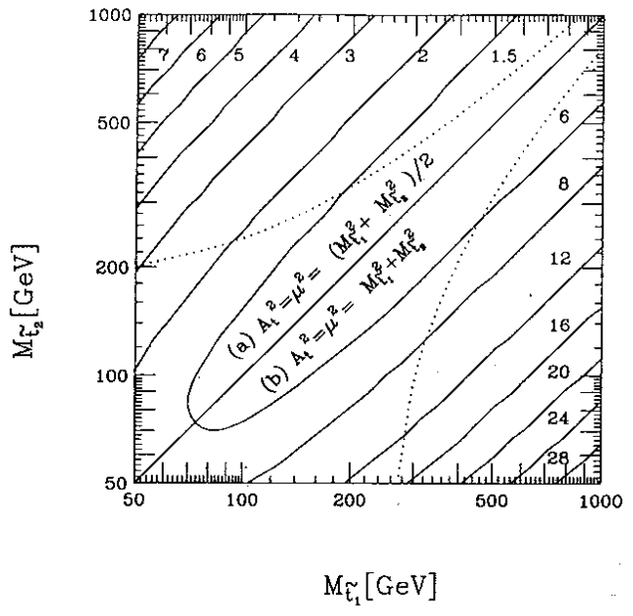

Fig. 1. Contours of constant $(\Delta m_0)^{\tilde{t}}$ in the $M_{\tilde{t}_1}$—$M_{\tilde{t}_2}$ plane. The trilinear mass parameters are (a) $\mu^2 = A_t^2 = \frac{1}{2}(M_{\tilde{t}_1}^2 + M_{\tilde{t}_2}^2)$ and (b) $\mu^2 = A_t^2 = M_{\tilde{t}_1}^2 + M_{\tilde{t}_2}^2$ and the mass of the top-quark is $m_t = 2m_Z$. The area between the dotted curves is forbidden by Eq. (7).

$$\begin{aligned} G(M_{\tilde{t}_1}^2, M_{\tilde{t}_2}^2, m_{h^0}^2) &= \left(\frac{M_{\tilde{t}_1}^2 + M_{\tilde{t}_2}^2}{M_{\tilde{t}_1}^2 - M_{\tilde{t}_2}^2} \right)^2 \left[\left(\frac{M_{\tilde{t}_1}^2 + M_{\tilde{t}_2}^2}{M_{\tilde{t}_1}^2 - M_{\tilde{t}_2}^2} \right) \ln \left(\frac{M_{\tilde{t}_1}^2}{M_{\tilde{t}_2}^2} \right) - 2 \right] + \mathcal{O}\left(\frac{m_{h^0}^2}{M_{\tilde{t}_1}^2} \right) \\ &= \tfrac{2}{3} + \mathcal{O}\left(\frac{M_{\tilde{t}_1}^2 - M_{\tilde{t}_2}^2}{M_{\tilde{t}_1}^2 + M_{\tilde{t}_2}^2} \right). \end{aligned} \tag{9}$$

In fig. 1 we have plotted contours of constant mass shift for two sets of parameters for μ and A_t. Here we have used the fact that f and therefore $(\Delta m_0)^{\tilde{t}}$ are symmetric under the interchange $M_{\tilde{t}_1} \leftrightarrow M_{\tilde{t}_2}$. Thus we have combined two parameter choices into one figure by plotting one choice above the diagonal and the other choice below the diagonal. In the upper triangle (a), we have set $\mu^2 = A_t^2 = \frac{1}{2}(M_{\tilde{t}_1}^2 + M_{\tilde{t}_2}^2)$ and $m_t = 2m_Z$. Here the contours are at $(\Delta m_0)^{\tilde{t}} = 1.5, 2, 3, \ldots$ GeV. In the lower triangle

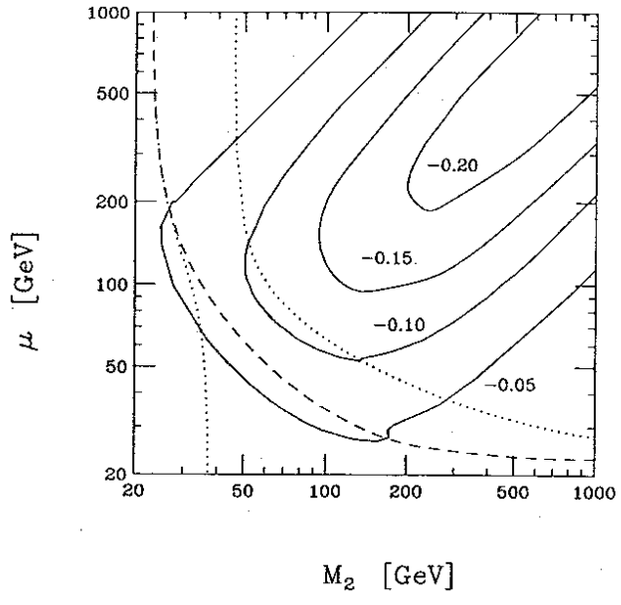

Fig. 2. Contours for $(\Delta m_0)^{\widetilde{\chi}} = -50, -100, -150$ and -200 MeV in the M_2—μ plane. The second Gaugino mass parameter is fixed by the grand unification relation ($M_1 = 5/3 \tan^2\theta_W M_2$). We have imposed the experimental constraint on the lower limit of the Higgs masses (*i.e.* $m_{A^0} + m_{h^0} = m_Z$).

(b), with $\mu^2 = A_t^2 = M_{\tilde{t}_1}^2 + M_{\tilde{t}_2}^2$ and the same value of m_t we have the same contour lines, but the labels are $(\Delta m_0)^{\widetilde{t}} = 6, 8, 12, 16, \ldots$ GeV. The area between the dotted curves in fig 1 is ruled out by the constraint in Eq. (7). The result for an arbitrary set of parameters can be obtained trivially by using the proportionality relations in Eq. (8). Note that the shapes of the contours stay the same as can be seen by comparing (a) and (b) [only the labels change by a factor of 4 and the area ruled out by Eq. (7) increases]. For example, if we had chosen $\mu^2 = A_t^2 = 2(M_{\tilde{t}_1}^2 + M_{\tilde{t}_2}^2)$ in fig. 1(a) or (b), the mass shift $(\Delta m_0)^{\widetilde{t}}$ would be multiplied by a factor of 16 or 4, respectively, and the labels would be 24, 32, 48, 64,... GeV. Mass shifts larger than $m_Z/2$ simply mean that $m_{A^0} > m_Z$ for arbitrary values of m_{h^0} and thus the non-observation of the process $Z \to A^0 h^0$ experimentally does *not* impose a lower limit on m_{h^0}.

In the chargino-neutralino sector we choose M_2 and μ as the only independent parameters (in grand unified theories: $M_1 = 5/3 \tan^2\theta_W M_2$). In fig. 2 we have

plotted contours of constant mass shift $(\Delta m_0)^{\widetilde{\chi}}$. We see that the shift is negative and very small [the plotted contours are at $(\Delta m_0)^{\widetilde{\chi}} = -50, -100, -150$ and -200 MeV]. The dotted (dashed) curves display the cases where one of the neutralino (chargino) masses becomes half the Higgs masses. It is interesting to note that the contours can develop small cusps when they cross the dashed curves or – much less significant – the dotted curves.

We conclude that large trilinear squark interactions can have a significant impact on the Higgs phenomenolgy of the MSSM and should not be neglected.

3. Supersymmetric Threshold Corrections to the Higgs Sector

In section 2 we have demonstrated the significance of non-logarithmic corrections in a particular case. In this section, we generalize this analysis to arbitrary values of $\tan\beta$. These corrections are embedded into the leading log analysis of ref. 15 and 16. We shall therefore begin with a brief review of the renormalization group technique used to obtain the leading log corrections.

Let Φ_1 and Φ_2 denote two complex $Y = 1$, $SU(2)_L$ doublet scalar fields. We introduce the notation

$$\Phi_n = \begin{pmatrix} H_n^+ \\ (H_n^0 + iA_n^0)/\sqrt{2} \end{pmatrix} . \tag{10}$$

The most general gauge invariant scalar potential is given by

$$\begin{aligned} \mathcal{V} = {} & m_{11}^2 \Phi_1^\dagger \Phi_1 + m_{22}^2 \Phi_2^\dagger \Phi_2 - [m_{12}^2 \Phi_1^\dagger \Phi_2 + \text{h.c.}] \\ & + \tfrac{1}{2}\lambda_1 (\Phi_1^\dagger \Phi_1)^2 + \tfrac{1}{2}\lambda_2 (\Phi_2^\dagger \Phi_2)^2 + \lambda_3 (\Phi_1^\dagger \Phi_1)(\Phi_2^\dagger \Phi_2) + \lambda_4 (\Phi_1^\dagger \Phi_2)(\Phi_2^\dagger \Phi_1) \\ & + \left\{ \tfrac{1}{2}\lambda_5 (\Phi_1^\dagger \Phi_2)^2 + [\lambda_6 (\Phi_1^\dagger \Phi_1) + \lambda_7 (\Phi_2^\dagger \Phi_2)] \Phi_1^\dagger \Phi_2 + \text{h.c.} \right\} . \end{aligned} \tag{11}$$

The fields will develop non-zero vacuum expectation values (VEVs) if the mass matrix m_{ij}^2 has at least one negative eigenvalue. The electrically neutral and CP-conserving minimum of the potential is

$$\langle \Phi_1 \rangle = \frac{1}{\sqrt{2}} \begin{pmatrix} 0 \\ v_1 \end{pmatrix} , \qquad \langle \Phi_2 \rangle = \frac{1}{\sqrt{2}} \begin{pmatrix} 0 \\ v_2 \end{pmatrix} , \tag{12}$$

where the v_i can be chosen to be real. The VEVs have been normalized so that $m_W^2 = \frac{1}{4} g_2^2 (v_1^2 + v_2^2)$. It is convenient to introduce the following notation

$$v^2 \equiv v_1^2 + v_2^2 , \qquad t_\beta \equiv \tan\beta \equiv v_2/v_1 . \tag{13}$$

The gauge symmetry will then be broken spontaneously. As a result three of the eight degrees of freedom of the original Higgs doublets are eaten by the $W^\pm$ and Z. The

remaining five physical Higgs particles are: two CP-even scalars (H^0 and h^0, with $m_{h^0} \leq m_{H^0}$), one CP-odd scalar (A^0) and a charged Higgs pair ($H^\pm$). The mass parameters m_{11} and m_{22} can be eliminated by imposing the minimization conditions and m_{12} can be replaced in terms of m_{A^0}. We find the following expressions for the charged Higgs mass and the neutral CP-even Higgs boson mass matrix

$$
\begin{aligned}
m^2_{H^\pm} &= m^2_{A^0} + \tfrac{1}{2}v^2(\lambda_5 - \lambda_4)\,, \\
\mathcal{M}^2 &= m^2_{A^0}\begin{pmatrix} s^2_\beta & -s_\beta c_\beta \\ -s_\beta c_\beta & c^2_\beta \end{pmatrix} \\
&\quad + v^2\begin{pmatrix} \lambda_1 c^2_\beta + 2\lambda_6 s_\beta c_\beta + \lambda_5 s^2_\beta & (\lambda_3+\lambda_4)s_\beta c_\beta + \lambda_6 c^2_\beta + \lambda_7 s^2_\beta \\ (\lambda_3+\lambda_4)s_\beta c_\beta + \lambda_6 c^2_\beta + \lambda_7 s^2_\beta & \lambda_2 s^2_\beta + 2\lambda_7 s_\beta c_\beta + \lambda_5 c^2_\beta \end{pmatrix}.
\end{aligned} \tag{14}
$$

The CP-even Higgs mass eigenvalues and the mixing angle α are

$$
m^2_{H^0,h^0} = \tfrac{1}{2}\left\{ \mathrm{tr}\,\mathcal{M}^2 \pm \sqrt{[\mathrm{tr}\,\mathcal{M}^2]^2 - 4\det\mathcal{M}^2} \right\}, \tag{15}
$$

$$
\begin{aligned}
\sin 2\alpha &= \frac{2\mathcal{M}^2_{12}}{\sqrt{[\mathrm{tr}\,\mathcal{M}^2]^2 - 4\det\mathcal{M}^2}}\,, \\
\cos 2\alpha &= \frac{\mathcal{M}^2_{11} - \mathcal{M}^2_{22}}{\sqrt{[\mathrm{tr}\,\mathcal{M}^2]^2 - 4\det\mathcal{M}^2}}\,.
\end{aligned} \tag{16}
$$

The phenomenology of the two-Higgs doublet model depends in detail on the various couplings of the Higgs bosons to gauge bosons, Higgs bosons and fermions. The Higgs couplings to gauge bosons follow from gauge invariance and are thus model independent. For example, the coupling of the two CP-even Higgs bosons to W and Z pairs is given in terms of the angles α and β by

$$
\begin{aligned}
g_{h^0VV} &= g_V m_V \sin(\beta-\alpha) \\
g_{H^0VV} &= g_V m_V \cos(\beta-\alpha)\,,
\end{aligned} \tag{17}
$$

where $g_V \equiv g_2\,[g_2/\cos\theta_W]$ for $V = W\,[Z]$. (In our notation, $g_1 \equiv g'$ and $g_2 \equiv g$.) There are no tree-level couplings of A^0 or $H^\pm$ to VV. Gauge invariance also

determines the strength of the trilinear couplings of one gauge boson to two Higgs bosons. For example,

$$
\begin{aligned}
g_{h^0A^0Z} &= \frac{g_2\cos(\beta-\alpha)}{2\cos\theta_W}\,, \\
g_{H^0A^0Z} &= \frac{-g_2\sin(\beta-\alpha)}{2\cos\theta_W}\,.
\end{aligned} \tag{18}
$$

The pattern of couplings of h^0 and H^0 to $W^\pm H^\mp$ is similar. For a complete set of Feynman rules for the couplings of Higgs bosons with gauge bosons and fermions in the two Higgs model see *e.g.* ref. 20. Finally, the 3-point and 4-point Higgs self-couplings depend on the two-Higgs-doublet potential [Eq. (11)]. The Feynman rules for the most important trilinear Higgs vertices are listed below

$$
\begin{aligned}
g_{h^0A^0A^0} &= \frac{2m_W}{g_2}\big[\lambda_1 s^2_\beta c_\beta s_\alpha - \lambda_2 c^2_\beta s_\beta c_\alpha - \widetilde{\lambda}_3(s^3_\beta c_\alpha - c^3_\beta s_\alpha) + 2\lambda_5 s_{\beta-\alpha} \\
&\qquad - \lambda_6 s_\beta(\epsilon_\beta s_{\alpha+\beta} + s_\alpha c_{2\beta}) - \lambda_7 c_\beta(c_\alpha c_{2\beta} - s_\beta s_{\alpha+\beta})\big]\,, \\
g_{H^0A^0A^0} &= \frac{-2m_W}{g_2}\big[\lambda_1 s^2_\beta c_\beta c_\alpha + \lambda_2 c^2_\beta s_\beta s_\alpha + \widetilde{\lambda}_3(s^3_\beta s_\alpha + c^3_\beta c_\alpha) - 2\lambda_5 c_{\beta-\alpha} \\
&\qquad - \lambda_6 s_\beta(c_\beta c_{\alpha+\beta} + c_\alpha c_{2\beta}) + \lambda_7 c_\beta(s_\beta c_{\alpha+\beta} + s_\alpha c_{2\beta})\big]\,, \\
g_{H^0h^0h^0} &= \frac{-6m_W}{g_2}\big[\lambda_1 s^2_\alpha c_\beta c_\alpha + \lambda_2 c^2_\alpha s_\beta s_\alpha + \widetilde{\lambda}_3(s^3_\alpha s_\beta + c^3_\alpha c_\beta - \tfrac{2}{3}c_{\beta-\alpha}) \\
&\qquad - \lambda_6 s_\alpha(c_\beta c_{2\alpha} + c_\alpha c_{\alpha+\beta}) + \lambda_7 c_\alpha(s_\beta c_{2\alpha} + s_\alpha c_{\alpha+\beta})\big]\,, \\
g_{H^0H^+H^-} &= g_{H^0A^0A^0} - \frac{2m_W}{g_2}(\lambda_5 - \lambda_4)c_{\beta-\alpha}\,, \\
g_{h^0H^+H^-} &= g_{h^0A^0A^0} - \frac{2m_W}{g_2}(\lambda_5 - \lambda_4)s_{\beta-\alpha}\,.
\end{aligned} \tag{19}
$$

In the MSSM, the effective Higgs self couplings λ_i at and above M_{SUSY} can be obtained by imposing the supersymmetric conditions

$$
\begin{aligned}
\lambda_1 &= \lambda_2 = \tfrac{1}{4}(g^2_2 + g^2_1)\,, \\
\lambda_3 &= \tfrac{1}{4}(g^2_2 - g^2_1)\,, \\
\lambda_4 &= -\tfrac{1}{2}g^2_2\,, \\
\lambda_5 &= \lambda_6 = \lambda_7 = 0\,.
\end{aligned} \tag{20}
$$

Furthermore, in unbroken SUSY we have $m^2_{11} = m^2_{22} = |\mu|^2$ and $m^2_{12} = 0$. However, with the soft SUSY breaking terms the mass parameters become arbitrary.

The parameters of any theory will, in general, depend on the energy scale ($\sqrt{s}$) at which they are evaluated. This dependence is described by the renormalization group equations (RGEs)

$$\frac{\mathrm{d}p_i}{\mathrm{d}t} = \beta_i(p_1, p_2, ..) \,, \qquad \text{where } t \equiv \ln(s) \,. \tag{21}$$

Here the parameters p_i stand for the Yukawa couplings h_f ($f = u, d, \ell$), the gauge couplings of the $SU(3)_C \times SU(2)_L \times U(1)_Y$ gauge group g_i ($i = 1, 2, 3$), the Higgs self-coupling constants λ_j ($j = 1, ..., 7$) and the mass parameters of the Higgs bosons m_{ij}^2 ($i, j = 1, 2$). At an intermediate scale $\sqrt{s}$ (for $m_Z < \sqrt{s} < M_{\rm SUSY}$) the gauge coupling constants and the self-coupling constants will evolve differently.#1

We begin by running the gauge coupling constants from the electroweak scale (where they are measured) up to $M_{\rm SUSY}$. At this scale, the SUSY boundary conditions given by Eq. (20) can be imposed, and we obtain the values of the Higgs self coupling constants λ_i at $M_{\rm SUSY}$. Next we determine the low energy effective coupling constants $\lambda_i(M_{\rm weak})$ by integrating the corresponding RGEs[22,23] from $M_{\rm SUSY}$ down to $M_{\rm weak}$. Finally, using $\lambda_i \equiv \lambda_i(M_{\rm weak})$ in Eqs. (14)–(19), we find the RGE-improved Higgs masses and trilinear interactions. By using the running parameters of the theory evaluated at the electroweak scale ($M_{\rm weak}$), we have incorporated the leading logarithmic radiative corrections to the Higgs parameters summed to all orders in perturbation theory.

The results obtained in this manner depend logarithmically on the soft SUSY-breaking mass parameters. This behavior is in excellent agreement with the full one-loop results in the limit $M_{\rm SUSY} \gg m_Z$. However, the leading log results are completely independent of the values of any trilinear Higgs-squark-squark interaction terms (*i.e.*, A-parameters and μ). These interactions contribute to the renormalization of λ_i via triangle diagrams, box diagrams, and wave function renormalization [depicted schematically in fig. 3]. These contributions to the quartic Higgs self couplings vanish in the limit $s \gg M_{\rm SUSY}$ and converge to a constant in the limit $s \ll M_{\rm SUSY}$. On a logarithmic scale they are therefore well approximated by a step function. These corrections can be incorporated into the leading log analysis by shifting the boundary conditions for the λ_i at $M_{\rm SUSY}$ by a finite amount

$$\lambda_i(M_{\rm SUSY}) = \lambda_i({\rm SUSY}) + \Delta\lambda_i^{(2)} + \Delta\lambda_i^{(3)} + \Delta\lambda_i^{(4)} \,. \tag{22}$$

Here $\lambda_i({\rm SUSY})$ are the scalar self-couplings of the unbroken supersymmetric theory given in Eq. (20) evaluated at $M_{\rm SUSY}$ and $\Delta\lambda_i^{(n)}$ ($n = 2, 3, 4$) are the results of the

#1 In refs. 4–6 and 21, it was assumed that $m_{A^0} \simeq M_{\rm SUSY}$, in which case the effective low-energy theory consists of the non-supersymmetric SM with one physical Higgs boson. Our approach extends the results of these authors by allowing for the possibility that all five physical Higgs states (h^0, H^0, A^0 and $H^\pm$) may have masses substantially below $M_{\rm SUSY}$.

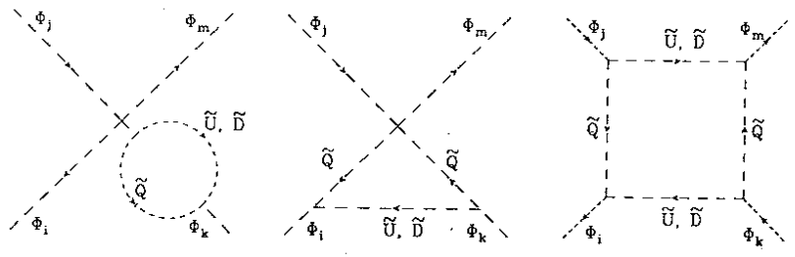

Fig. 3. Wave function renormalization, triangle and box diagrams contributing to the low energy effective coupling constants λ_i ($i = 1, ..7$).

wave function renormalization, triangle diagrams and box diagrams shown in fig. 3, respectively.

Here we will present result for the special case of $M_{\rm SUSY} \equiv M_{\widetilde{Q}} = M_{\widetilde{U}} = M_{\widetilde{D}}$. The general formulae are shown in Appendix B. The results for the triangle diagrams (with two powers of trilinear coupling constants A_U, A_D or μ) denoted by a superscript (3) are

$$\begin{aligned}
64\pi^2 M_{\rm SUSY}^2 \Delta\lambda_1^{(3)} &= N_c \left\{ A_D^2 h_D^2 \left(8h_D^2 - g_2^2 - g_1^2\right) + \mu^2 h_U^2 \left(g_2^2 + g_1^2\right) \right\} , \\
64\pi^2 M_{\rm SUSY}^2 \Delta\lambda_2^{(3)} &= N_c \left\{ A_U^2 h_U^2 \left(8h_U^2 - g_2^2 - g_1^2\right) + \mu^2 h_D^2 \left(g_2^2 + g_1^2\right) \right\} , \\
64\pi^2 M_{\rm SUSY}^2 \Delta\lambda_3^{(3)} &= N_c \Big\{ 2\mu^2 \left(h_U^2 - h_D^2\right)^2 + 2h_U^2 h_D^2 \left(A_U + A_D\right)^2 \\
&\qquad + \tfrac{1}{2}\left(g_1^2 - g_2^2\right) \left[\left(A_D^2 - \mu^2\right) h_D^2 + \left(A_U^2 - \mu^2\right) h_U^2 \right] \Big\} , \\
64\pi^2 M_{\rm SUSY}^2 \Delta\lambda_4^{(3)} &= N_c \Big\{ 2\mu^2 \left(h_U^2 + h_D^2\right)^2 - 2h_U^2 h_D^2 \left(A_U + A_D\right)^2 \\
&\qquad + g_2^2 \left[\left(A_D^2 - \mu^2\right) h_D^2 + \left(A_U^2 - \mu^2\right) h_U^2 \right] \Big\} , \\
128\pi^2 M_{\rm SUSY}^2 \Delta\lambda_5^{(3)} &= 0 \,, \\
128\pi^2 M_{\rm SUSY}^2 \Delta\lambda_6^{(3)} &= N_c \left\{ A_D h_D^2 \left(g_2^2 + g_1^2 - 8h_D^2\right) - A_U h_U^2 \left(g_2^2 + g_1^2\right) \right\} , \\
128\pi^2 M_{\rm SUSY}^2 \Delta\lambda_7^{(3)} &= N_c \left\{ A_U h_U^2 \left(g_2^2 + g_1^2 - 8h_U^2\right) - A_D h_D^2 \left(g_2^2 + g_1^2\right) \right\} ,
\end{aligned} \tag{23}$$

and the results for the box diagrams (with four powers of A_U, A_D or μ) denoted with a superscript (4) are

$$\begin{aligned}
96\pi^2 M_{\rm SUSY}^4 \Delta\lambda_1^{(4)} &= -N_c \left\{ A_D^4 h_D^4 + \mu^4 h_U^4 \right\} , \\
96\pi^2 M_{\rm SUSY}^4 \Delta\lambda_2^{(4)} &= -N_c \left\{ A_U^4 h_U^4 + \mu^4 h_D^4 \right\} ,
\end{aligned}$$

$$
\begin{aligned}
96\pi^2 M_{\rm SUSY}^4 \Delta\lambda_3^{(4)} &= -N_c\left\{\mu^2(A_U^2 h_U^4 + A_D^2 h_D^4) + h_U^2 h_D^2(\mu^2 - A_U A_D)^2\right\}\,,\\
96\pi^2 M_{\rm SUSY}^4 \Delta\lambda_4^{(4)} &= -N_c\left\{\mu^2(A_U^2 h_U^4 + A_D^2 h_D^4) - h_U^2 h_D^2(\mu^2 - A_U A_D)^2\right\}\,,\\
96\pi^2 M_{\rm SUSY}^4 \Delta\lambda_5^{(4)} &= -N_c\mu^2\left\{A_D^2 h_D^4 + A_U^2 h_U^4\right\}\,,\\
96\pi^2 M_{\rm SUSY}^4 \Delta\lambda_6^{(4)} &= \;\; N_c\mu\left\{\mu^2 A_U h_U^4 + A_D^3 h_D^4\right\}\,,\\
96\pi^2 M_{\rm SUSY}^4 \Delta\lambda_7^{(4)} &= \;\; N_c\mu\left\{\mu^2 A_D h_D^4 + A_U^3 h_U^4\right\}\,.
\end{aligned}
\tag{24}
$$

Finally, the self energy diagrams yield corrections to the kinetic term of the Higgs fields which have to be absorbed by redefining the Higgs fields

$$
\Phi_i \to \widehat{\Phi}_i \equiv (\delta_{ij} - \tfrac{1}{2}A'_{ij})\,\Phi_j \qquad \text{where} \qquad A'_{ij} \equiv \left.\frac{{\rm d}A_{\Phi_i\Phi_j}(p^2)}{{\rm d}p^2}\right|_{p^2=0}\,. \tag{25}
$$

The contributions to the A'_{ij} coming from the trilinear scalar interactions are given by

$$
A'_{ij} = -\frac{N_c}{96\pi^2 M_{\rm SUSY}^2}\left[h_U^2\begin{pmatrix}\mu^2 & -\mu A_U\\ -\mu A_U & A_U^2\end{pmatrix} + h_D^2\begin{pmatrix}A_D^2 & -\mu A_D\\ -\mu A_D & \mu^2\end{pmatrix}\right]. \tag{26}
$$

If we then express the quartic terms of the potential in terms of the new fields $\widehat{\Phi}$ we obtain

$$
\begin{aligned}
\Delta\lambda_1^{(2)} &= \tfrac{1}{2}(g_1^2+g_2^2)A'_{11}\,,\\
\Delta\lambda_2^{(2)} &= \tfrac{1}{2}(g_1^2+g_2^2)A'_{22}\,,\\
\Delta\lambda_3^{(2)} &= -\tfrac{1}{4}(g_1^2-g_2^2)(A'_{11}+A'_{22})\,,\\
\Delta\lambda_4^{(2)} &= -\tfrac{1}{2}g_2^2(A'_{11}+A'_{22})\,,\\
\Delta\lambda_5^{(2)} &= 0\,,\\
\Delta\lambda_6^{(2)} &= \tfrac{1}{8}(g_1^2+g_2^2)A'_{12}\,,\\
\Delta\lambda_7^{(2)} &= \tfrac{1}{8}(g_1^2+g_2^2)A'_{12}\,,
\end{aligned}
\tag{27}
$$

where we have used the (supersymmetric) tree-level results for the λ_i that appeared on the right hand side of Eqs. (27) evaluated at the scale $M_{\rm SUSY}$. All the coupling constants of the right hand sides of Eqs. (23), (24) and (27) are evaluated at the scale $M_{\rm SUSY}$.

The low-energy effective Higgs potential $\mathcal{V}$ is given in Eq. (11). Here the low energy effective coupling constants $\lambda_i \equiv \lambda_i(M_{\rm weak})$ are obtained by solving the RGEs [Eq. (21)] subject to the supersymmetric boundary conditions [Eq. (22)]. We can now compute the mass eigenvalues, mixing angles and coupling constants in Eq. (14)–(19) numerically. Note, that this analysis also includes all higher order terms proportional to $\Delta\lambda_i[g_2^2\ln(M_{\rm SUSY}^2/M_{\rm weak}^2)]^n$ $(1 \le n < \infty)$. However, before presenting the numerical results of this analysis we shall first look at a few analytic results.

At the one-loop level, the effects of shifting the boundary conditions [Eq. (22)] are simply additive. Thus, if we denote the one-loop leading log squared mass shifts by $(\Delta m^2)_{\rm 1LL}$ then we obtain the following expressions for the neutral Higgs masses in the limit of large $\tan\beta$ and for $m_{A^0} < m_Z$

$$
\begin{aligned}
\left(m_{H^0}^2 - m_Z^2\right)_{\beta=\pi/2} = (\Delta m_{h^0}^2)_{\rm 1LL} &- \frac{N_c g_2^2 m_W^2}{96\pi^2 M_{\rm SUSY}^4}\left[\left(\frac{A_t m_t}{s_\beta m_W}\right)^4 + \left(\frac{\mu m_b}{c_\beta m_W}\right)^4\right]\\
&+ \frac{N_c g_2^2 m_W^2}{96\pi^2 M_{\rm SUSY}^2}\left[12\frac{A_t^2 m_t^4}{s_\beta^4 m_W^4} - 4\frac{A_t^2 m_t^2}{s_\beta^2 m_W^2 c_W^2} + 2\frac{\mu^2 m_b^2}{c_\beta^2 m_W^2 c_W^2}\right]\,,
\end{aligned}
\tag{28}
$$

and

$$
\left(m_{h^0}^2 - m_{A^0}^2\right)_{\beta=\pi/2} = -\frac{N_c g_2^2 \mu^2}{96\pi^2 M_{\rm SUSY}^4}\left(\frac{A_t^2 m_t^4}{s_\beta^4 m_W^2} + \frac{A_b^2 m_b^4}{c_\beta^4 m_W^2}\right)\,. \tag{29}
$$

If $m_{A^0} > m_Z$ then interchange m_{h^0} and m_{H^0}. Taking the limit $\beta \to \pi/2$ on the right hand side of Eqs. (28) and (29) is subtle because of factors of c_β in the denominator. The appropriate limit is one where the Yukawa coupling $h_b \equiv g_2 m_b/(\sqrt{2}m_W c_\beta)$ is fixed. Thus, in the limit $\beta \to \pi/2$, it follows that $m_b \to 0$ such that m_b/c_β is fixed. We also refrain from setting $s_\beta = 1$ to preserve the symmetry of the formulae above.

As a second example consider the radiative corrections to charged Higgs mass sum rule. Those corrections have already been obtained in refs. 24–27 and serve as a useful check of our formalism. Define

$$
\Delta m_{H^\pm}^2 \equiv m_{H^\pm}^2 - m_{A^0}^2 - m_W^2\,, \tag{30}
$$

so that $\Delta m_{H^\pm}^2 = 0$ at tree-level. We then find

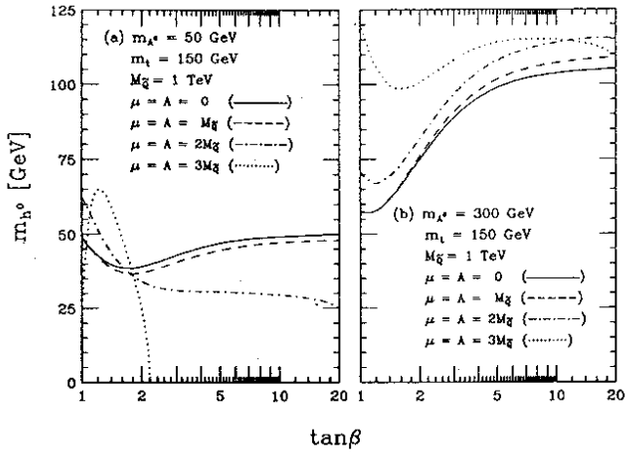

Fig. 4. The neutral Higgs mass m_{h^0} as a function of $\tan\beta$ for (a) $m_{A^0} = 50$ GeV and (b) $m_{A^0} = 300$ GeV, for $m_t = 150$ GeV and $M_{\tilde{Q}} = M_{\rm SUSY} = 1$ TeV. All A-parameters are taken to be equal ($A = A_t = A_b$); the four contours shown correspond to $\mu = A = 0$, 1, 2 and 3 TeV, respectively.

$$\Delta m^2_{H^\pm} = (\Delta m^2_{H^\pm})_{\rm 1LL} + \frac{N_c g_2^2 m_W^2}{96\pi^2}\left[\frac{m_t^2}{m_W^2 s_\beta^2}\left(\frac{\mu^2 - 2A_t^2}{M^2_{\rm SUSY}}\right) + \frac{m_b^2}{m_W^2 c_\beta^2}\left(\frac{\mu^2 - 2A_b^2}{M^2_{\rm SUSY}}\right)\right]$$
$$+\frac{N_c g_2^2 m_W^2}{64\pi^2}\left[\frac{m_t^2 m_b^2}{m_W^4 s_\beta^2 c_\beta^2}\left(\frac{A_t + A_b}{M^2_{\rm SUSY}}\right)^2 - \frac{\mu^2}{M^2_{\rm SUSY}}\left(\frac{m_t^2}{m_W^2 s_\beta^2} + \frac{m_b^2}{m_W^2 c_\beta^2}\right)^2\right]$$
$$-\frac{N_c g_2^2 m_t^2 m_b^2}{192\pi^2 m_W^2 s_\beta^2 c_\beta^2}\left(\frac{A_t A_b - \mu^2}{M^2_{\rm SUSY}}\right)^2, \qquad (31)$$

where $(\Delta m^2_{H^\pm})_{\rm 1LL}$ is the one-loop leading log result. This result agrees with the full one-loop calculation presented in ref. 26. Under the assumption that all the soft-supersymmetry-breaking parameters are of the same order and $\tan\beta \ll m_t/m_b$, the dominant contribution to $\Delta m^2_{H^\pm}$ is

$$\Delta m^2_{H^\pm} = -\frac{N_c g_2^2 m_W^2}{64\pi^2}\left(\frac{\mu}{M_{\rm SUSY}}\right)^2\left(\frac{m_t}{s_\beta m_W}\right)^4 + \mathcal{O}\left(g_2^2 m_t^2\right). \qquad (32)$$

For sufficiently large μ, this correction dominates the leading log contributions which grow only as m_t^2.

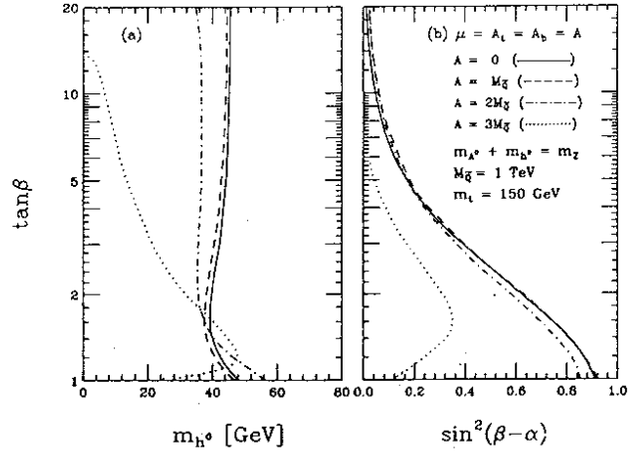

Fig. 5. As a function of $\tan\beta$, we plot (a) the neutral Higgs mass m_{h^0} and (b) the factor $\sin^2(\beta - \alpha)$ for $m_t = 150$ GeV and $M_{\tilde{Q}} = M_{\rm SUSY} = 1$ TeV. All A-parameters are taken to be equal ($A = A_t = A_b$); the four curves shown correspond to $\mu = A = 0$, 1, 2 and 3 TeV, respectively. The sum $m_{A^0} + m_{h^0} = m_Z$ is kept fixed in both plots.

We now proceed to evaluate the radiative corrections to the Higgs masses and couplings. These have been computed by numerically solving the RGEs for the Higgs self-coupling parameters to determine the $\lambda_i(M_{\rm weak})$ as described above. These results are then inserted into Eqs. (14)–(19) to obtain the radiatively corrected Higgs masses and couplings. In all numerical results presented in this paper we shall take the squark mass parameters to be equal to a common soft SUSY-breaking mass $M_{\tilde{Q}} = M_{\tilde{D}} = M_{\tilde{U}} = M_{\rm SUSY}$.

In fig. 4 we plot the Higgs mass m_{h^0} as a function of $\tan\beta$ for $m_t = 150$ GeV and for two choices of m_{A^0}. All A-parameters are taken to be equal. The four curves shown correspond to $\mu = A = 0, 1, 2$ and 3 TeV, respectively. The behavior of m_{h^0} at large values of $\tan\beta$ is noteworthy; for $m_{A^0} \lesssim m_Z$, we see that m_{h^0} decreases monotonically with A. In contrast, in the case $m_{A^0} \gtrsim m_Z$ and large $\tan\beta$, m_{h^0} initially increases, reaches a maximum at $A \approx \sqrt{6} M_{\rm SUSY}$, and then falls off rapidly. These behaviors can be obtained immediately from Eqs. (28) and (29). Some of the implications for Higgs phenomenology at LEP have already been discussed in section 2 [see also ref. 28]. In fig. 5 we plot the Higgs mass m_{h^0} and the factor $\sin^2(\beta - \alpha)$ as functions of $\tan\beta$ for $m_t = 150$ GeV and $M_{\rm SUSY} = 1$ TeV. We fix the sum $m_{A^0} + m_{h^0} = m_Z$ in both plots in order to bound m_{h^0} while keeping $Z \to A^0 h^0$ kinematically forbidden. Fig. 5(a) displays contours of fixed $m_{A^0} + m_{h^0} = m_Z$. To the left (right) of these contours, $Z \to A^0 h^0$ is kinematically allowed (forbidden). In

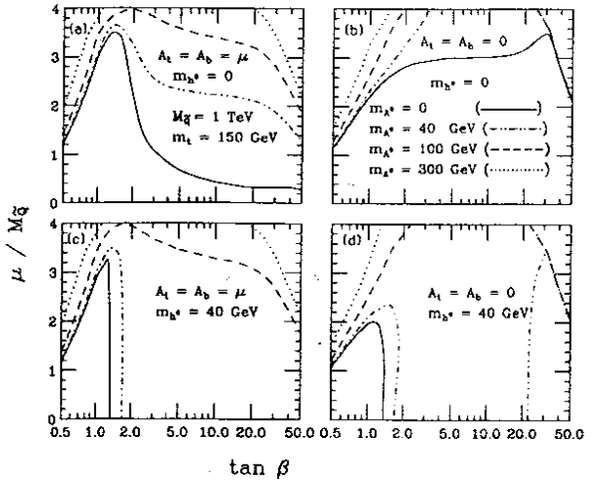

Fig. 6. Contours of constant $m_{A^o} = 0$, 40, 100 and 300 GeV in the μ–tanβ plane for $m_t = 150$ GeV, $M_{\tilde{Q}} = M_{\rm SUSY} = 1$ TeV. In (a) and (b) $m_{h^o} = 0$ for two choices of the A parameters, respectively. In (c) and (d) $m_{h^o} = 40$ GeV.

fig. 5(b) we see that the decay $Z \to Z^* h^0$, with a rate proportional to $\sin^2(\beta - \alpha)$, can be sufficiently suppressed in the large tanβ regime to escape detection. On the other hand, the rate for $Z \to A^0 h^0$ is proportional to $\cos^2(\beta - \alpha)$ which is near unity for large tanβ and $m_{A^o} \lesssim m_Z$. Thus, $Z \to A^0 h^0$ would be observed in this regime unless it is kinematically forbidden. In the absence of the Higgs discovery at LEP, we can therefore conclude that the parameter regime to the left of the respective curves (for various choices of $\mu = A$) shown in fig. 5(a) are excluded. On the other hand, at large tanβ, the parameter regime to the right of the respective curves cannot be ruled out based on current LEP data. In particular, for large $\mu = A$ (and for large tanβ), the true experimental lower limit on m_{h^o} [*i.e.*, the dotted curve of fig. 5(a)] can be significantly lower than the quoted Higgs mass limits of the LEP detector collaborations [17–19] as we have pointed out in section 2. For an A-parameter of the order of $3M_{\rm SUSY}$ one can easily get in conflict with constraints coming from the stability of the electroweak vacuum[29]. However, comparison with the full one-loop results of section 2 tells us that radiative corrections as large as the ones presented in figs. 4 and 5 can already be obtained for much smaller values of A_t, A_b and μ due to a logarithmic enhancement factor [of the order of $\ln(M^2_{\tilde{t}_1}/M^2_{\tilde{t}_2})$] in the case large squark mass splitting.

In the analysis presented in this section, predictions for the (radiatively corrected) Higgs masses are obtained as a function of the soft SUSY breaking parameters. However, not all choices of these parameters lead to physically (or phenomenologically)

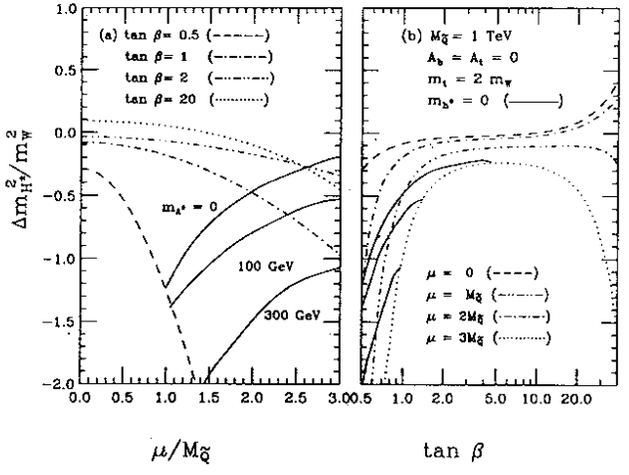

Fig. 7. The shift in the charged Higgs squared mass, $\Delta m^2_{H^\pm}$, normalized to m^2_W as a function of μ and tanβ for $m_t = 2m_W$ and $M_{\tilde{Q}} = M_{\rm SUSY} = 1$ TeV. The A-parameters are set to zero. In our RGE analysis $\Delta m^2_{H^\pm}$ is independent of m_{A^o}. In addition, we depict in (a) and (b) solid curves corresponding to $m_{h^o} = 0$ which depend on m_{A^o} as indicated in (a).

sensible results. For example, consider the cases of $m_t = 150$ GeV, $M_{\rm SUSY} = 1$ TeV and $m_{A^o} = 0$, 40, 100 or 300 GeV. Then the condition $m_{h^o} > 0$ (or $m_{h^o} > 40$ GeV if we take recent LEP limits at face values) rules out the parameter region above the solid, dashed or dot-dashed curves in fig. 6.

Finally, we consider the corrections to the charged Higgs mass sum rule. In figs. 7–9 we plot the shift in the charged Higgs squared mass due to radiative corrections, $\Delta m^2_{H^\pm}$ [see Eq. (30)], as a function of tanβ for various choices of A and μ. We choose $m_t = 2m_W$ and $M_{\tilde{Q}} = M_{\rm SUSY} = 1$ TeV. Note that in our RGE analysis $\Delta m^2_{H^\pm}$ is independent of m_{A^o}. For large values of tanβ (say, $m_b \tan\beta \gtrsim m_W$) the leading log term proportional to $m_t^2 m_b^2/(m_W^2 s_\beta^2 c_\beta^2)$ dominates and causes $m_{H^\pm}$ to increase above its tree-level value (except in certain cases where the effects of squark mixing become very significant). For more moderate values of tanβ, a different term in the leading log radiative corrections, proportional to m_t^2/s_β^2 lowers $m_{H^\pm}$ below its tree-level value. In addition, there is a negative contribution to $\Delta m^2_{H^\pm}$ proportional to m_t^4 due to squark-mixing [see Eq. (32)]. As a result, there exists a regime in the SUSY parameter space where $\Delta m^2_{H^\pm} < -m^2_W$ [see figs. 7 and 9] which would imply that $m_{H^\pm} < m_{A^o}$. For example, for $m_t = 2m_W$, tan$\beta = 1$ and $\mu = 2.5 M_{\rm SUSY}$, we find $m_{H^\pm} \approx m_{A^o}$. Note that the radiative corrections in the neutral Higgs sector can

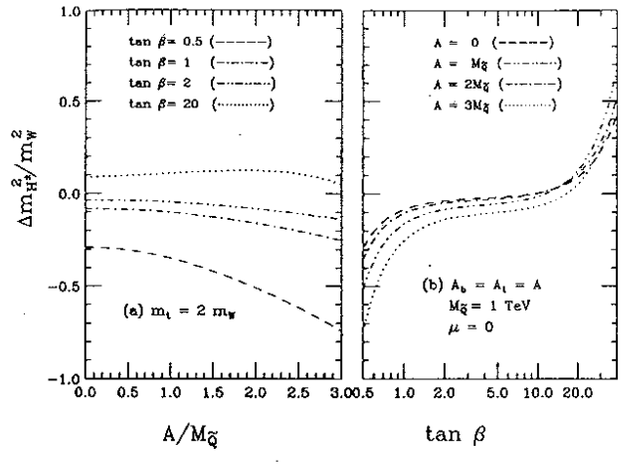

Fig. 8. The shift in the charged Higgs squared mass, $\Delta m^2_{H\pm}$, normalized to m^2_W as a function of (a) the A-parameter and (b) $\tan\beta$ for $m_t = 2m_W$ and $M_{\widetilde{Q}} = M_{\rm SUSY} = 1$ TeV. The parameter μ is set to zero.

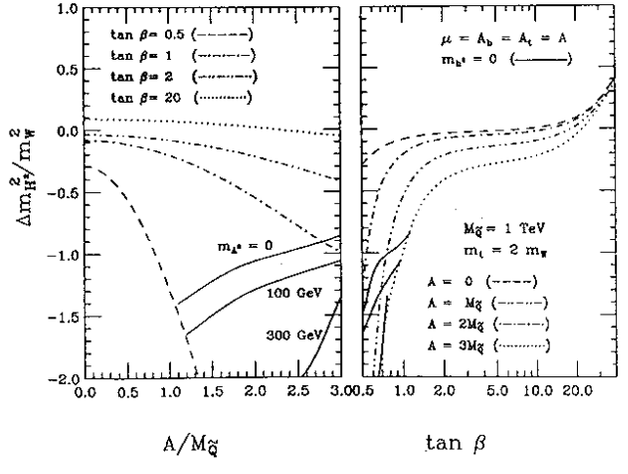

Fig. 9. The shift in the charged Higgs squared mass, $\Delta m^2_{H\pm}$, normalized to m^2_W as a function of (a) $A = A_t = A_b = \mu$ and (b) $\tan\beta$ for $m_t = 2m_W$ and $M_{\widetilde{Q}} = M_{\rm SUSY} = 1$ TeV. In our RGE analysis $\Delta m^2_{H\pm}$ is independent of m_{A°. In addition, we depict in (a) and (b) solid curves corresponding to $m_{h^\circ} = 0$ which depend on m_{A° as indicated in (a).

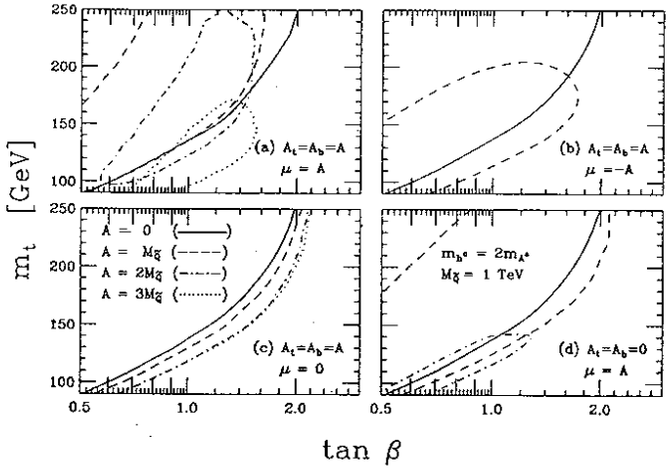

Fig. 10. The range of parameters in the $\tan\beta$–m_t plane where $m_{h^\circ} = 2m_{A^\circ} = 40$ GeV for various choices of μ and the A-parameters, and $M_{\rm SUSY} = M_{\widetilde{Q}} = 1$ TeV.

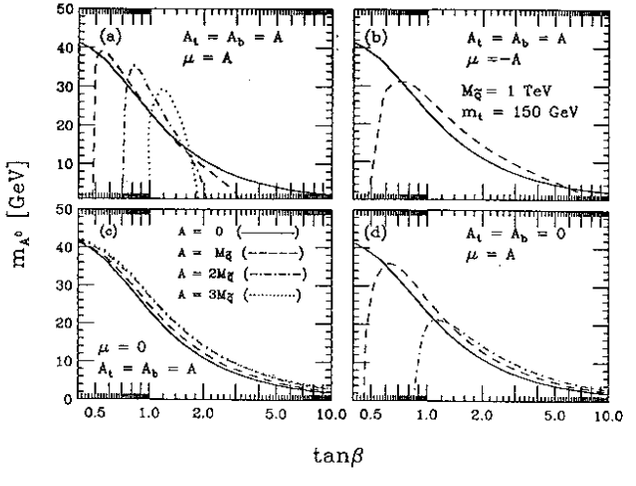

Fig. 11. The range of parameters in the $\tan\beta$–m_{A° plane where $m_{h^\circ} = 2m_{A^\circ}$ and $m_t = 150$ GeV for various choices of μ and the A-parameters, and $M_{\rm SUSY} = M_{\widetilde{Q}} = 1$ TeV.

impose constraints on the parameter space [see fig. 6] that depend on m_{A^0}. These constraints rule out the area below and to the right of the solid curves in figs. 7 and 9.

When the radiative corrections are included, the tree-level inequality $m_{h^0} \leq m_{A^0}|\cos 2\beta|$ is no longer satisfied. In particular, it is possible to have $m_{h^0} \geq 2m_{A^0}$, in which case the decay $h^0 \to A^0A^0$ is kinematically allowed with decay width

$$\Gamma(h^0 \to A^0A^0) = \frac{g^2_{h^0A^0A^0}}{32\pi m_{h^0}}\left(1 - \frac{4m^2_{A^0}}{m^2_{h^0}}\right)^{1/2}, \tag{33}$$

where the coupling constant $g_{h^0A^0A^0}$ is given by Eq. (19). In ref. 25 and 12 it has been shown that the process $h^0 \to A^0A^0$ is the dominant decay mode in most of the parameter space where the decay is kinematically allowed. Thus, the most important effects of the radiative corrections will be the modification of the parameter space where the decay is kinematically allowed.

In figs. 10 and 11, we depict the region of parameter space where $m_{h^0} \geq 2m_{A^0}$. As before, all A-parameters are taken to be equal. We exhibit curves corresponding to various choices of A and μ, for $M_{\tilde{Q}} = M_{\rm SUSY} = 1$ TeV. The parameter space where $h^0 \to A^0A^0$ is kinematically allowed lies to the left of [or within] the displayed curves.

4. Conclusion

We have presented the dominant non-leading log radiative corrections to the Higgs sector of the MSSM. These corrections are generated by trilinear Higgs-squark-squark interactions at the SUSY threshold.

A full one-loop computation has been performed in the large $\tan\beta$ limit. In this limit, one can derive an experimental lower limits of the sum of the CP-even and CP-odd Higgs masses from non-observation of the decay $Z \to A^0h^0$. In the MSSM, a global U(1) symmetry in the limit $\tan\beta \to \infty$ causes A^0 and h^0 to be mass degenerate at tree-level. Kinematics set the following lower limit on the individual Higgs masses: $m_{h^0} > m_Z/2 + (\Delta m_0)$ and $m_{A^0} > m_Z/2 - (\Delta m_0)$, where the mass shift (Δm_0) is a model-dependent quantity. We have computed the one-loop radiative corrections to (Δm_0) in the MSSM in the limit $\tan\beta \to \infty$ which is zero at tree-level.

We have seen that the only place where a negative mass shift can be generated is the Higgsino sector. Contributions from this sector are well below 1 GeV for a Higgs mass of the order of half the Z-boson mass and for the mass parameters μ and M_2 anywhere below 1 TeV. Thus the experimental lower limit of m_{A^0} is not significantly altered by the inclusion of radiative corrections.

On the other hand, in the squark-sector corrections are of the order of a few GeV for the natural choice $\mu^2 = A_t^2 = \frac{1}{2}(M^2_{\tilde{t}_1} + M^2_{\tilde{t}_2})$ and $m_t = 2m_Z$. These corrections grow with the fourth power of m_t, with the second power of μ and A_t and logarithmically

with the squark mass ratio $M_{\tilde{t}_1}/M_{\tilde{t}_2}$. Thus, if we increase A_t and μ by a factor of 2 the mass shift increases by a factor of 16 and leaves no experimental lower limit on m_{h^0} coming from the Z-width in most parts of the $M_{\tilde{t}_1}$—$M_{\tilde{t}_2}$ plane. [The inclusion of the bottom squark can supply an additional factor of up to 2 in the case of degenerate bottom- and top Yukawa couplings.]

Even though we have done this calculation in the limit $\tan\beta \to \infty$, our conclusions are valid as long as $\tan\beta \gg 1$. Moreover, this corresponds precisely to the parameter regime in which the lower limits on m_{h^0} are derived from the process $Z \to A^0h^0$. Therefore it seems impossible to use non-observation of this process to set any lower limits on m_{h^0} even for arbitrary $\tan\beta$ without restricting the magnitude of the parameters m_t, μ and A_t.

In our numerical analysis of the Higgs sector for arbitrary $\tan\beta$, we have focused on the case where all the supersymmetric partners are approximately mass degenerate. Leading logarithms summed to all orders in perturbation theory are included by solving the RGEs numerically. Non-leading logarithmic corrections due to squark mixing effects are incorporated by computing the Higgs 4-point functions at the SUSY threshold and modifying the supersymmetric boundary condition.

We find that the upper limit for m_{A^0} for which the decay $h^0 \to A^0A^0$ is kinematically allowed can increase by a few GeV. Our results for the charged Higgs sector can be summarized as follows: The leading log corrections to $m_{H^\pm}$ only grow with m_t^2. However, there are non-logarithmic contributions due to squark mixing effects that grow as m_t^4. These effects could (in extreme cases) yield $m_{H^\pm} \lesssim m_{A^0}$.

Acknowledgement

Most of this work was carried out in collaboration with Howard Haber. I would like to thank the organizers of this workshop for their invitation and hospitality.

This work was supported in part by the United States Department of Energy.

APPENDIX A: Exact One-loop Corrections for $m_{A^0} - m_{h^0}$

The results are presented in terms of the following integrals

$$B_0(q^2, m_1^2, m_2^2) = -16\pi^2 i \int \frac{\mathrm{d}^{2\omega}k}{(2\pi)^{2\omega}} (k^2 - m_1^2 + i\epsilon)^{-1} [(k+q)^2 - m_2^2 + i\epsilon]^{-1}$$
$$= \Delta - \int_0^1 \mathrm{d}x \ln\left[m_2^2 x + m_1^2(1-x) - q^2 x(1-x)\right] . \qquad \text{(A.1)}$$

Here we have defined

$$\Delta \equiv (4\pi)^{2-\omega}\Gamma(2-\omega) = \frac{1}{2-\omega} - \gamma_{\mathrm{E}} + \ln(4\pi) , \qquad \text{(A.2)}$$

where γ_{E} is the Euler constant. In order to derive asymptotic results we expand Eq. (A.1) in powers of the momentum q^2

$$B_0(q^2, m_1^2, m_2^2) = \Delta - \frac{m_1^2 \ln m_1^2 - m_2^2 \ln m_2^2}{m_1^2 - m_2^2} + 1 + \mathcal{O}\left(\frac{q^2}{m_1^2 + m_2^2}\right) \qquad \text{(A.3)}$$

All the results below are given in the $\tan\beta \to \infty$ limit.

(a) The Contributions from the Squarks

The contribution from the top-squarks are given by

$$(\Delta m_0^2)^{\tilde{t}} = \frac{N_c g^2 m_t^2}{64\pi^2 m_W^2} \mu^2 \sin^2 2\theta_t \, (B_{11} + B_{22} - 2B_{12})$$
$$= \frac{N_c g^2 m_Z^2}{4\pi^2 c_W^2} \left(\frac{m_t}{2m_Z}\right)^4 \left(\frac{2\mu^2}{M_{\tilde{t}_1}^2 + M_{\tilde{t}_2}^2}\right) \left(\frac{2A_t^2}{M_{\tilde{t}_1}^2 + M_{\tilde{t}_2}^2}\right) G(M_{\tilde{t}_1}^2, M_{\tilde{t}_2}^2, m_{h^0}^2) , \qquad \text{(A.4)}$$

where we have used the short-hand notation $B_{ij} \equiv B_0(m_{h^0}^2, M_{\tilde{t}_i}^2, M_{\tilde{t}_j}^2)$ and

$$G(M_{\tilde{t}_1}^2, M_{\tilde{t}_2}^2, m_{h^0}^2) \equiv \left(\frac{M_{\tilde{t}_1}^2 + M_{\tilde{t}_2}^2}{M_{\tilde{t}_1}^2 - M_{\tilde{t}_2}^2}\right)^2 (B_{11} + B_{22} - 2B_{12}) . \qquad \text{(A.5)}$$

The bottom-squark contribution is obtained by replacing $m_t \to m_b$, $\theta_t \to \theta_b$ and $A_t \to \mu$. Keep in mind that the product $\tan\beta m_b$ stays finite if we keep the bottom Yukawa coupling fixed (which in this limit is more sensible than keeping m_b fixed).

(b) The Contribution from the Charginos

The contribution from the charginos are given by

$$(\Delta m_0^2)^{\chi^\pm} = -\frac{g^2}{4\pi^2} \sum_{i,j=1}^{2} (Q_{ij} Q_{ji} + \text{h.c.}) \, m_{\chi_i^\pm} m_{\chi_j^\pm} B_{ij} \qquad \text{(A.6)}$$

where $B_{ij} \equiv B_0(m_{h^0}^2, m_{\chi_i^\pm}^2, m_{\chi_j^\pm}^2)$ and the chargino mass eigenvalues $m_{\chi_j^\pm}$ and the vertices Q are given by

$$Q_{ij} = \frac{1}{\sqrt{2}} V_{i1} U_{j2} , \qquad \text{(A.7)}$$

where the mass eigenvalues m_χ and the unitary matrices U and V that diagonalize the mass matrix are defined as in ref. 20 and 30.

(c) The Contribution from the Neutralinos

The contribution from the neutralinos are given by

$$(\Delta m_0^2)^{\chi^0} = -\frac{g^2}{8\pi^2} \sum_{i,j=1}^{4} (Q''_{ij} Q''_{ji} + \text{h.c.}) \, m_{\chi_i^0} m_{\chi_j^0} B_{ij} , \qquad \text{(A.8)}$$

where the neutralino mass eigenvalues $m_{\chi_i^0}$ and the unitary matrix Z that diagonalizes the mass matrix are defined as in ref. 20 and 30.

$$Q''_{ij} = \tfrac{1}{2} \left[Z_{i3} \left(Z_{j2} - Z_{j1} \tan\theta_W \right) + Z_{j3} \left(Z_{i2} - Z_{i1} \tan\theta_W \right) \right] . \qquad \text{(A.9)}$$

APPENDIX B: Radiative Corrections due to Trilinear Higgs-Squark-Squark Interactions

In this appendix we present the radiative corrections to the Higgs self couplings due to soft squark interactions for arbitrary squark masses. The one–loop radiative corrections can be absorbed into the tree–level potential by shifting the tree-level parameters as seen in Eq. (22). The results for the shifts $\Delta\lambda_i^{(3)}$ coming from the triangle diagrams are

$$
\begin{aligned}
32\pi^2\Delta\lambda_1^{(3)} &= \frac{4N_c h_D^4 A_D^2}{M_{\widetilde{Q}}^2 - M_{\widetilde{D}}^2}\ln\left(\frac{M_{\widetilde{Q}}^2}{M_{\widetilde{D}}^2}\right) \\
&+N_c h_U^2\mu^2\left[g_2^2 f(M_{\widetilde{U}}^2, M_{\widetilde{Q}}^2) - g_1^2\left(Y_U f(M_{\widetilde{U}}^2, M_{\widetilde{Q}}^2) + Y_Q f(M_{\widetilde{Q}}^2, M_{\widetilde{U}}^2)\right)\right] \\
&-N_c h_D^2 A_D^2\left[g_2^2 f(M_{\widetilde{D}}^2, M_{\widetilde{Q}}^2) + g_1^2\left(Y_D f(M_{\widetilde{D}}^2, M_{\widetilde{Q}}^2) + Y_Q f(M_{\widetilde{Q}}^2, M_{\widetilde{D}}^2)\right)\right], \qquad \text{(B.1)}
\end{aligned}
$$

$$
\begin{aligned}
32\pi^2\Delta\lambda_2^{(3)} &= \frac{4N_c h_U^4 A_U^2}{M_{\widetilde{Q}}^2 - M_{\widetilde{U}}^2}\ln\left(\frac{M_{\widetilde{Q}}^2}{M_{\widetilde{U}}^2}\right) \\
&-N_c h_U^2 A_U^2\left[g_2^2 f(M_{\widetilde{U}}^2, M_{\widetilde{Q}}^2) - g_1^2\left(Y_U f(M_{\widetilde{U}}^2, M_{\widetilde{Q}}^2) + Y_Q f(M_{\widetilde{Q}}^2, M_{\widetilde{U}}^2)\right)\right] \\
&+N_c h_D^2\mu^2\left[g_2^2 f(M_{\widetilde{D}}^2, M_{\widetilde{Q}}^2) + g_1^2\left(Y_D f(M_{\widetilde{D}}^2, M_{\widetilde{Q}}^2) + Y_Q f(M_{\widetilde{Q}}^2, M_{\widetilde{D}}^2)\right)\right], \qquad \text{(B.2)}
\end{aligned}
$$

$$
\begin{aligned}
16\pi^2\left(\Delta\lambda_3^{(3)} + \Delta\lambda_4^{(3)}\right) &= \frac{4N_c h_D^4\mu^2}{M_{\widetilde{Q}}^2 - M_{\widetilde{D}}^2}\ln\left(\frac{M_{\widetilde{Q}}^2}{M_{\widetilde{D}}^2}\right) + \frac{4N_c h_U^4\mu^2}{M_{\widetilde{Q}}^2 - M_{\widetilde{U}}^2}\ln\left(\frac{M_{\widetilde{Q}}^2}{M_{\widetilde{U}}^2}\right) \\
&+N_c h_U^2\left(A_U^2 - \mu^2\right)\left[g_2^2 f(M_{\widetilde{U}}^2, M_{\widetilde{Q}}^2) - g_1^2\left(Y_U f(M_{\widetilde{U}}^2, M_{\widetilde{Q}}^2) + Y_Q f(M_{\widetilde{Q}}^2, M_{\widetilde{U}}^2)\right)\right] \\
&+N_c h_D^2\left(A_D^2 - \mu^2\right)\left[g_2^2 f(M_{\widetilde{D}}^2, M_{\widetilde{Q}}^2) + g_1^2\left(Y_D f(M_{\widetilde{D}}^2, M_{\widetilde{Q}}^2) + Y_Q f(M_{\widetilde{Q}}^2, M_{\widetilde{D}}^2)\right)\right], \qquad \text{(B.3)}
\end{aligned}
$$

$$
\begin{aligned}
32\pi^2\Delta\lambda_4^{(3)} &= N_c h_U^2\left[\left(2h_U^2 - g_2^2\right)\mu^2 - \left(2h_D^2 - g_2^2\right)A_U^2\right] f(M_{\widetilde{U}}^2, M_{\widetilde{Q}}^2) \\
&+ N_c h_D^2\left[\left(2h_D^2 - g_2^2\right)\mu^2 - \left(2h_U^2 - g_2^2\right)A_D^2\right] f(M_{\widetilde{D}}^2, M_{\widetilde{Q}}^2) \\
&+4N_c h_D^2 h_U^2\left(\frac{\mu^2 - A_U A_D}{M_{\widetilde{U}}^2 - M_{\widetilde{D}}^2}\right)\left[\left(M_{\widetilde{U}}^2 - M_{\widetilde{Q}}^2\right) f(M_{\widetilde{U}}^2, M_{\widetilde{Q}}^2) - \left(\widetilde{U} \to \widetilde{D}\right)\right], \qquad \text{(B.4)}
\end{aligned}
$$

$$
32\pi^2\Delta\lambda_5^{(3)} = 0\,, \qquad \text{(B.5)}
$$

$$
\begin{aligned}
32\pi^2\Delta\lambda_6^{(3)} &= -\frac{4N_c h_D^4\mu A_D}{M_{\widetilde{Q}}^2 - M_{\widetilde{D}}^2}\ln\left(\frac{M_{\widetilde{Q}}^2}{M_{\widetilde{D}}^2}\right) \\
&-N_c h_U^2\mu A_U\left[g_2^2 f(M_{\widetilde{U}}^2, M_{\widetilde{Q}}^2) - g_1^2\left(Y_U f(M_{\widetilde{U}}^2, M_{\widetilde{Q}}^2) + Y_Q f(M_{\widetilde{Q}}^2, M_{\widetilde{U}}^2)\right)\right] \\
&+N_c h_D^2\mu A_D\left[g_2^2 f(M_{\widetilde{D}}^2, M_{\widetilde{Q}}^2) + g_1^2\left(Y_D f(M_{\widetilde{D}}^2, M_{\widetilde{Q}}^2) + Y_Q f(M_{\widetilde{Q}}^2, M_{\widetilde{D}}^2)\right)\right], \qquad \text{(B.6)}
\end{aligned}
$$

$$
\begin{aligned}
32\pi^2\Delta\lambda_7^{(3)} &= -\frac{4N_c h_U^4\mu A_U}{M_{\widetilde{Q}}^2 - M_{\widetilde{U}}^2}\ln\left(\frac{M_{\widetilde{Q}}^2}{M_{\widetilde{U}}^2}\right) \\
&+N_c h_U^2\mu A_U\left[g_2^2 f(M_{\widetilde{U}}^2, M_{\widetilde{Q}}^2) - g_1^2\left(Y_U f(M_{\widetilde{U}}^2, M_{\widetilde{Q}}^2) + Y_Q f(M_{\widetilde{Q}}^2, M_{\widetilde{U}}^2)\right)\right] \\
&-N_c h_D^2\mu A_D\left[g_2^2 f(M_{\widetilde{D}}^2, M_{\widetilde{Q}}^2) + g_1^2\left(Y_D f(M_{\widetilde{D}}^2, M_{\widetilde{Q}}^2) + Y_Q f(M_{\widetilde{Q}}^2, M_{\widetilde{D}}^2)\right)\right], \qquad \text{(B.7)}
\end{aligned}
$$

where we have defined

$$
f(M_1^2, M_2^2) = \frac{1}{M_1^2 - M_2^2}\left[1 - \frac{M_1^2}{M_1^2 - M_2^2}\ln\left(\frac{M_1^2}{M_2^2}\right)\right]. \qquad \text{(B.8)}
$$

Note that all the effects discussed in this appendix are proportional to the Yukawa couplings and thus only the third generation is relevant for our analysis. The results for the shifts $\Delta\lambda_i^{(4)}$ due to the box diagrams are

$$
\begin{aligned}
16\pi^2\Delta\lambda_1^{(4)} &= N_c h_U^4\mu^4 g(M_{\widetilde{Q}}^2, M_{\widetilde{U}}^2) + N_c h_D^4 A_D^4 g(M_{\widetilde{Q}}^2, M_{\widetilde{D}}^2), \\
16\pi^2\Delta\lambda_2^{(4)} &= N_c h_U^4 A_U^4 g(M_{\widetilde{Q}}^2, M_{\widetilde{U}}^2) + N_c h_D^4\mu^4 g(M_{\widetilde{Q}}^2, M_{\widetilde{D}}^2), \\
8\pi^2\left(\Delta\lambda_3^{(4)} + \Delta\lambda_4^{(4)}\right) &= N_c h_U^4\mu^2 A_U^2 g(M_{\widetilde{Q}}^2, M_{\widetilde{U}}^2) + N_c h_D^4\mu^2 A_D^2 g(M_{\widetilde{Q}}^2, M_{\widetilde{D}}^2), \\
16\pi^2\lambda_4^{(4)} &= -N_c h_U^2 h_D^2\left(\mu^2 - A_U A_D\right)^2\left(\frac{f(M_{\widetilde{U}}^2, M_{\widetilde{Q}}^2) - f(M_{\widetilde{D}}^2, M_{\widetilde{Q}}^2)}{M_{\widetilde{U}}^2 - M_{\widetilde{D}}^2}\right) \\
&+ N_c h_U^4 A_U^2\mu^2 g(M_{\widetilde{U}}^2, M_{\widetilde{Q}}^2) + N_c h_D^4 A_D^2\mu^2 g(M_{\widetilde{D}}^2, M_{\widetilde{Q}}^2),
\end{aligned}
$$

$$16\pi^2\Delta\lambda_5^{(4)} = N_c h_U^4 \mu^2 A_U^2 g(M_{\tilde{Q}}^2, M_{\tilde{U}}^2) + N_c h_D^4 \mu^2 A_D^2 g(M_{\tilde{Q}}^2, M_{\tilde{D}}^2)\,,$$

$$16\pi^2\Delta\lambda_6^{(4)} = -N_c h_U^4 \mu^3 A_U g(M_{\tilde{Q}}^2, M_{\tilde{U}}^2) - N_c h_D^4 \mu A_D^3 g(M_{\tilde{Q}}^2, M_{\tilde{D}}^2)\,,$$

$$16\pi^2\Delta\lambda_7^{(4)} = -N_c h_U^4 \mu A_U^3 g(M_{\tilde{Q}}^2, M_{\tilde{U}}^2) - N_c h_D^4 \mu^3 A_D g(M_{\tilde{Q}}^2, M_{\tilde{D}}^2)\,, \qquad \text{(B.9)}$$

where we have defined

$$g(M_1^2, M_2^2) \equiv G(M_1^2, M_2^2, 0)(M_1^2 + M_2^2)^{-2} \equiv \frac{f(M_1^2, M_2^2) - f(M_2^2, M_1^2)}{M_1^2 - M_2^2}\,. \qquad \text{(B.10)}$$

Next we present the radiative corrections to the quadratic terms due to soft interaction terms. Corrections of this type are frequently ignored[31] since the momentum independent pieces can be absorbed by redefining the arbitrary mass parameters. However, there are pieces proportional to p^2 (p_μ is the momentum) that renormalize the kinetic term and therefore the propagator. Wave function renormalization is required in order to return the kinetic term and therefore the propagator into its canonical form. This can be seen by expanding the Higgs self energies [see also Eq. (25)]

$$A_{\Phi_i\Phi_j}(p^2) = A_{\Phi_i\Phi_j}(0) + p^2 A'_{ij}(0) + \mathcal{O}\left(\frac{p^2}{M_{\rm SUSY}^2}\right)\,, \qquad \text{(B.11)}$$

Note that the only divergence generated by trilinear interactions is contained in $A_{\Phi_i\Phi_j}(0)$ and can be absorbed into the arbitrary mass matrix m_{ij}^2. Clearly, the piece proportional to p^2 renormalizes the kinetic term. This term can be brought into its canonical form by redefining the fields Φ as in Eq. (25). The contributions of the soft squark interactions to the derivative of the Higgs self-energies is

$$A'_{ij} = -\frac{N_c h_U^2 h(M_{\tilde{Q}}^2, M_{\tilde{U}}^2)}{32\pi^2 M_{\rm SUSY}^2} \begin{pmatrix} \mu^2 & -\mu A_U \\ -\mu A_U & A_U^2 \end{pmatrix} + (U \to D, A \leftrightarrow \mu)\,, \qquad \text{(B.12)}$$

where we defined the function

$$h(M_1^2, M_2^2) \equiv \frac{M_1^2 f(M_1^2, M_2^2) - M_2^2 f(M_2^2, M_1^2)}{M_1^2 - M_2^2}\,. \qquad \text{(B.13)}$$

It is important to note that there is *no* renormalization of the gauge fields (*i.e.* $A'_{VV} = 0$, $V = W, B$) an thus *no* renormalization of the gauge couplings.

The results in Eq. (23), (24) and (26) can be obtained by taking the limits

$$\lim_{M_2 \to M_1} f(M_1^2, M_2^2) = -\frac{1}{2M_1^2}\,,$$

$$\lim_{M_2 \to M_1} g(M_1^2, M_2^2) = -\frac{1}{6M_1^4}\,,$$

$$\lim_{M_2 \to M_1} f(M_1^2, M_2^2) = \frac{1}{3M_1^2}\,. \qquad \text{(B.14)}$$

REFERENCES

1. M.S. Berger, *Phys. Rev.* **D41** (1990) 225.
2. H.E. Haber and R. Hempfling, *Phys. Rev. Lett.* **66** (1991) 1815.
3. Y. Okada, M. Yamaguchi and T. Yanagida, *Prog. Theor. Phys.* **85** (1991) 1; J. Ellis, G. Ridolfi and F. Zwirner, *Phys. Lett.* **B257** (1991) 83.
4. R. Barbieri, M. Frigeni and F. Caravaglios *Phys. Lett.* **B258** (1991) 167.
5. Y. Okada, M. Yamaguchi and T. Yanagida, *Phys. Lett.* **B262** (1991) 54.
6. J.R. Espinosa and M. Quirós *Phys. Lett.* **B266** (1991) 389.
7. A. Yamada, *Phys. Lett.* **B263** (1991) 233.
8. P.H. Chankowski, S. Pokorski and J. Rosiek, *Phys. Lett.* **B274** (1992) 191; *Phys. Lett.* **B286** (1992) 307; A. Brignole, *Phys. Lett.* **B281** (1992) 284.
9. M.A. Díaz and H.E. Haber, *Phys. Rev.* **D46** (1992) 3086.
10. M. Drees and M.M. Nojiri, *Phys. Rev.* **D45** (1992) 2482.
11. H.E. Haber, SCIPP 92/11 (1992) to appear in the Proceedings of the International Workshop on Electroweak Symmetry Breaking, Hiroshima, Japan, 12-15 November 1991.
12. H.E. Haber, R. Hempfling and Y. Nir, *Phys. Rev.* **D46** (1992) 3015.
13. D.M. Pierce, A. Papadopoulos and S. Johnson, *Phys. Rev. Lett.* **68** (1992) 3678.
14. K. Sasaki, M. Carena and C.E.M. Wagner, *Nucl. Phys.* **B381** (1992) 66.
15. H.E. Haber and R. Hempfling, preprint SCIPP 91/33 (1992), to be published in *Phys. Rev.* **D**.
16. H.E. Haber, these proceedings.
17. D. Decamp *et al.* [ALEPH Collaboration], *Phys. Lett.* **B237** (1990) 291; P. Abreu *et al.* [DELPHI Collaboration], *Phys. Lett.* **B245** (1990) 276; *Nucl. Phys.* **B373** (1992) 3; B. Adeva *et al.* [L3 Collaboration], *Phys. Lett.* **B251** (1990) 311; M.Z. Akrawy *et al.* [OPAL Collaboration], *Z. Phys.* **C49** (1991) 1; P.D. Acton *et al.*, *Phys. Lett.* **B268** (1991) 122.

18. D. Decamp *et al.* [ALEPH Collaboration], *Phys. Lett.* **B265** (1991) 475.
19. K. Hisaka *et al.* [Particle Data Group], *Phys. Rev.* **D45** (1992) S1.
20. J.F. Gunion, H.E. Haber, G.L. Kane, and S. Dawson, *The Higgs Hunter's Guide,* (Addison-Wesley, Redwood City, CA, 1990).
21. R. Hempfling, in "*Phenomenological Aspects of Supersymmetry*", Lecture Notes on Physics, edited by W. Hollik, R. Rückl and J. Wess, (Springer-Verlag, 1992) p. 260-279 (1992).
22. T.P. Cheng, E. Eichten and L.-F. Li, *Phys. Rev.* **D9** (1974) 2259.
23. N. Cabibbo, L. Maiani, G. Parisi, R. Petronzio *Nucl. Phys.* **B158** (1979) 295.
24. J.F Gunion and A. Turski, *Phys. Rev.* **D39** (1989) 2701; **D40** (1989) 2333.
25. A. Brignole, J. Ellis, G. Rudolfi and F. Zwirner, *Phys. Lett.* **B271** (1991) 123; [E: **B273,** 550 (1991)].
26. M.A. Díaz and H.E. Haber, *Phys. Rev.* **D45** (1992) 4246.
27. A. Brignole, *Phys. Lett.* **B277** (1992) 313.
28. R. Hempfling, *Phys. Lett.* **B296** (1992) 121.
29. J.F. Gunion, H.E. Haber and M. Sher, *Nucl. Phys.* **B306** (1988) 1.
30. J.F. Gunion and H.E. Haber *Nucl. Phys.* **B272** (1986) 1; H.E Haber and G.L. Kane, *Phys. Rep.* **117** (1985) 75.
31. T. Moroi and Y. Okada, *Mod. Phys. Lett.* **A7** (1992) 187.